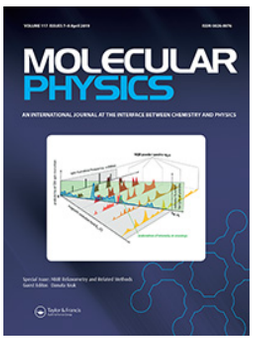

Taylor & Francis
Taylor & Francis Group

Molecular Physics

An International Journal at the Interface Between Chemistry and Physics

ISSN: 0026-8976 (Print) 1362-3028 (Online) Journal homepage: https://www.tandfonline.com/loi/tmph20

Relaxometric investigations addressing the determination of intracellular water lifetime: a novel tumour biomarker of general applicability

Maria Rosaria Ruggiero, Simona Baroni, Silvio Aime & Simonetta Geninatti Crich

To cite this article: Maria Rosaria Ruggiero, Simona Baroni, Silvio Aime & Simonetta Geninatti Crich (2019) Relaxometric investigations addressing the determination of intracellular water lifetime: a novel tumour biomarker of general applicability, Molecular Physics, 117:7-8, 968-974, DOI: 10.1080/00268976.2018.1527045

To link to this article: https://doi.org/10.1080/00268976.2018.1527045

Published online: 25 Sep 2018.

MOLECULAR PHYSICS
2019, VOL. 117, NOS. 7–8, 968–974
https://doi.org/10.1080/00268976.2018.1527045

Taylor & Francis
Taylor & Francis Group

NMR RELAXOMETRY AND RELATED METHODS

Relaxometric investigations addressing the determination of intracellular water lifetime: a novel tumour biomarker of general applicability

Maria Rosaria Ruggiero[a], Simona Baroni[a], Silvio Aime[a,b] and Simonetta Geninatti Crich[a]

[a]Department of Molecular Biotechnology and Health Sciences, University of Torino, Torino, Italy; [b]IBB-CNR, Torino, Italy

ABSTRACT

^{1}H Fast-Field Cycling NMR relaxometry is proposed as a powerful method to investigate tumour cell metabolism by measuring changes in cell water content and mobility across the cellular membrane. Measurements of intracellular water residence time in cultured cells were carried out by measuring T_1 at fixed field (0.2 T) after the addition of a paramagnetic Gd complex (Prohance) at different concentrations in the external medium. Investigations on tumour cells (mammary adenocarcinoma TS/A) grown in normo- or hypoxic conditions or suspended in 'hypo-osmotic' solutions allowed us to demonstrate that both hypoxic and hypo-osmotic conditions cause a marked increase in water mobility as assessed by the elongation of T_1. Conversely, the metabolic change caused by glutamine (an aminoacid essential for tumour growth) deprivation caused a water mobility decrease (shorter T_1). These findings suggest that T_1 measurements at low and variable magnetic field strengths, giving access to the assessment of intracellular water lifetime, can provide important information about tumour cell metabolism in real time and non-invasively.

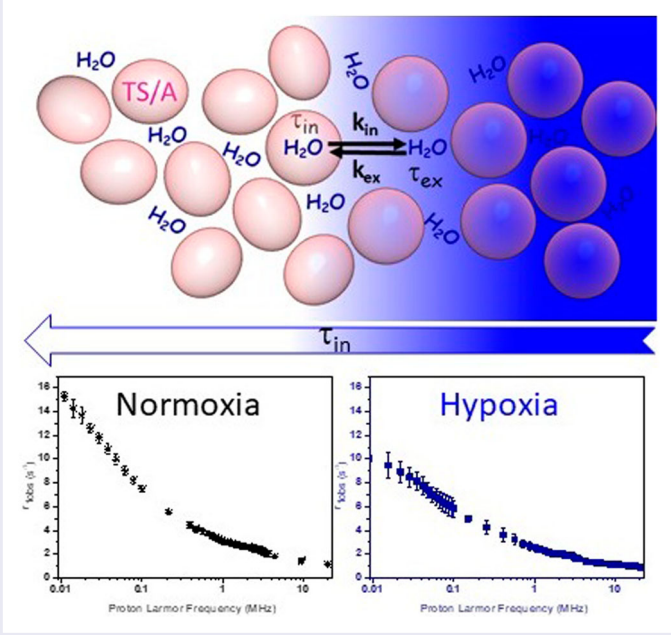

ARTICLE HISTORY
Received 2 July 2018
Accepted 14 September 2018

KEYWORDS
Nuclear Magnetic Resonance Profiles (NMRD); relaxometry; tumour metabolism; intracellular water lifetime; tumour hypoxia

1. Introduction

Intracellular water lifetime (τ_{in}) has been recently suggested as a new, promising cancer hallmark with the potential to discriminate metabolic and microenvironmental states of tumour cells and their changes with therapy [1]. Mammalian cells regulate their volume to prevent unintentional changes in intercellular signalling and cell metabolism. Intentional cell volume changes occur as cells undergo proliferation, apoptosis, or cell migration [2]. To regulate their volume, cells use a

CONTACT Simonetta Geninatti Crich simonetta.geninatti@unito.it Department of Molecular Biotechnology and Health Sciences, University of Torino, via Nizza 52, Torino 10126, Italy

number of channels and transport systems to flux osmolytes across the plasma membrane, thus yielding a concomitant movement of large quantities of water. It follows that the intracellular lifetime of water molecules (τ_{in}) is the result of several contributions, amongst which it is central the osmotically driven cytosolic membrane water crossing and the overexpression/upregulation of transporters such as GLUT-1, Na^+/K^+ ATP-ase and aquaporins [3]. Recently, we reported that the $1/T_1$ NMRD profiles measured in vivo on implanted mammary tumours unequivocally report on the change of water amount and mobility in the pathological tissues [4]. This result opens new horizons for the non-invasive evaluation of tumour metabolic phenotypes, by providing useful and more detailed information related to the metastatic propensity of the tumour. This finding prompted us to apply a parallel relaxometric methodology that allows the 'in vitro' measurements of τ_{in} of cultured cells eventually undergone to different stimuli. We expected that the acquisition of new data may shed light on the different mechanisms at the basis of τ_{in} changes. In this context, hypoxia appears as an important condition to be considered. In fact, hypoxia is a characteristic feature of various solid tumours and is exploited as a key marker for tumour progression and metastatic spread [5,6]. Moreover, hypoxia limits the efficacy of radio- and chemo-therapy and its changes can be used to monitor early responses to therapy. Currently, there is a great attention for diagnostic technologies able to report on the hypoxia status of cancer lesions, as it would enable clinical development of personalised, hypoxia-based therapies, which, likely, will ultimately improve outcomes. During anaerobic glycolysis, that occurs in solid tumours under hypoxic conditions, there is a significant increase of intracellular osmotic pressure due to the production of the high amount of lactate [7,8]. Thus, glucose metabolism provides cells with osmotic energy driving hydrodynamic work as well as the chemical energy that determine the rate of water exchange rate ($1/\tau_{in}$) across the cellular membrane. The other stimuli, herein considered, deals with cell starvation induced by glutamine (Gln) deprivation. In fact, recent studies on metabolism indicated that utilisation of Gln is critical in tumour growth, progression, and development [9]. Exogenous Gln represents an additional carbon source in cancer cells, to enhance the contribution arising from glycolytic metabolites for energy production. During the glycolytic process, Gln is converted to α-ketoglutarate by glutaminase and glutamate dehydrogenase, which maintains cell growth and survival through the tricarboxylic acid (TCA) cycle under glucose deprivation condition [10]. Under normal cell conditions, small amounts of Gln are consumed in macromolecule biosynthesis and energy formation. In this study, we aim at assessing changes in τ_{in} of cancer cells in response to the deprivation of Gln with the intent of developing a diagnostic test able to differentiate tumour from normal cells on the basis of their different response to the aminoacid deprivation. The quantitative determination of the cell membrane permeability of a murine breast cancer cell line (TS/A) [11,12] was carried out in vitro following an established relaxometric procedure [13–16]. For this purpose, measurements were carried out at the magnetic field of 0.5 T in the presence of increasing amounts (5–40 mM) of the paramagnetic Gd-HPDO3A complex in the extracellular space of cellular suspensions. Then, these results were validated with the acquisition of NMRD profiles of cellular pellets that may be considered a 'tissue like' slice of about 0.8 cm.

2. Material and methods

2.1. Cell cultures

TS/A (kindly provided by prof. F. Cavallo's group, University of Turin) were grown in RPMI 1640 medium supplemented with 10% fetal bovine serum (FBS), 100 U/mL Penicillin (P) with 100 μg/ml Streptomycin (S) and 4 mM Glutamine (Gln). Cells were cultured in 5% CO_2/95% air at 37°C in a humidified chamber and were split every 2–3 days. All cells were tested negative for mycoplasma by MycoAlert™ Mycoplasma Detection Kit. All materials were purchased from Lonza (Basel, Switzerland).

2.2. In vitro determination of membrane permeability

TS/A cells (7 million) were detached with 0.05% trypsin and 0.02% EDTA in PBS, washed once with PBS and re-suspended in the presence of variable concentrations of Gd-HPDO3A (5–40 mM in PBS), kindly provided by Bracco S.p.A. (Milan, Italy) [13]. Eu-HPDO3A was synthetised as described in [17]. The relaxometric measurements were carried out within 15 min. The cells were transferred in 5 mm NMR tubes and centrifuged 5 min at 0.1 rcf (4°C). The measurements of the cellular pellet were carried out at 0.5 T and 25°C on a Stelar SPINMASTER spectrometer (Stelar, Mede, Italy) by means of the inversion-recovery (IR) pulse sequence with 64 τ increments.

2.3. FFC-NMR profiles

For FFC-NMR profiles 50 million of TS/A cells were detached with 0.05% trypsin and 0.02% EDTA in PBS, washed once with PBS. The cells were re-suspended in

the presence of 1 ml of phosphate buffer and were transferred in 5 mm NMR tubes and centrifuged 15 min at 0.2 rcf (4°C). The ^{1}H profiles were measured over a continuum of magnetic field strength from 0.01 to 10 MHz proton Larmor frequency on the fast-field cycling relaxometer (SMARtracer^{TM}, Stelar (Mede, PV)) at 25°C. Used sequences were the Non Pre-Polarised (NP) sequence between 10 and 7 MHz and the Pre-Polarised (PP) sequence between 7 and 0.01 MHz [18]. The detection and polarisation fields are set at 7 and 9 MHz, respectively. T_1 was determined by the saturation recovery method. Sixteen values of delay time (τ) between pulses were used. The reproducibility of the T_1 data was ± 5%.

2.4. H&E staining

TS/A cells were seeded in glass bottom confocal dishes at a density of 50,000 of cells per well. After 24 h, they were fixed with methanol at 4°C for 10 min. The cells were incubated for 5 min in presence of haematoxylin and then washed with tap water until it became clear. Afterwards, they were incubated for 5 min in presence of eosin and then washed with tap water until it was clear. The images were acquired at 40× magnification on Leica 3000 microscope.

2.5. MRI

MR images at 1 T were acquired with an Aspect M2-High Performance MRI System (Aspect Magnet Technologies Ltd, Netanya, Israel) [19]. Glass capillaries containing about 2×10^6 cells were placed in an agar phantom and MR imaging was performed by using a standard T_1-weighted multislice spin-echo sequence (TR/TE/NEX = 800/8/4, FOV = 2.5 cm, NEX = number of excitations; FOV = field of view).

2.6. ICP-MS

The final Gd and Eu concentrations were determined by inductively coupled plasma mass spectrometry (ICP-MS) (Element-2; Thermo-Finnigan, Rodano (MI), Italy). Sample digestion was performed with 2 ml of concentrated HNO_3 (70%) under microwave heating (Milestone MicroSYNTH Microwave Labstation).

2.7. NMR measurements and data analysis

In a cell suspension, water molecules distribute in the extracellular (ex) space and in the intracellular (in) cytoplasm and exchange between the two compartments with a water exchange rate of efflux k_{in} ($= \tau_{\mathrm{in}}{}^{-1}$) and influx k_{ex} ($= \tau_{\mathrm{ex}}{}^{-1}$), respectively. These parameters are related by the equilibrium mass balance $k_{in} \cdot V_{in} = k_{ex} \cdot V_{ex}$, where V_{in} and V_{ex} ($= 1 - V_{in}$) are the intracellular and extracellular volume fraction, respectively.

$$H_2O_{ex} \underset{\tau_{in}^{-1}}{\overset{\tau_{ex}^{-1}}{\rightleftarrows}} H_2O_{in}$$

From the relaxometric point of view, each environment is characterised by its own longitudinal relaxation rate, the extracellular ($R_{1\mathrm{ex}}$) and the intracellular one ($R_{1\mathrm{in}}$), respectively.

In cell suspensions, without the addition of paramagnetic contrast agents (CA), water exchange between the two compartments occurs much faster than the recovery of magnetisation due to T_1, i.e. $k_{ex} + k_{in} >> |R_{1\mathrm{ex}} - R_{1\mathrm{in}}|$ (fast exchange limit). In this condition, water molecules visit both compartments multiple times over the magnetisation recovery. The time evolution of the magnetisation in the IR experiment is monoexponential and described by the following equation:

$$M_z = M_0 \cdot \{1 - 2 \cdot \exp[-t(V_{\mathrm{ex}} \cdot R_{1\mathrm{ex}} + V_{\mathrm{in}} \cdot R_{1\mathrm{in}})]\} \quad (1)$$

For the volume fraction determination, a 50 µM solution of Eu-HPDO3A complex was added to the cell suspension (see below). This complex does not affect the relaxation rate of the extracellular compartment where remain confined.

In the presence of a Gd-HPDO3A, confined into the extracellular space, the condition $k_{ex} + k_{in} \sim |R_{1\mathrm{ex}} - R_{1\mathrm{in}}|$ is met and the water exchange modulates the observed relaxation behaviour, that is described by the Bloch-McConnell equations [1,3,20]. The recovery of longitudinal magnetisation after inversion is no longer monoexponential (Figure 1) and is expressed as

$$M_z = M_0 \cdot \{1 - 2[(1 - a_S) \cdot \exp(-t \cdot R_{1L}) + a_S \cdot \exp(-t \cdot R_{1S})]\} \quad (2)$$

where M_z is the instantaneous magnetisation, M_0 is its Boltzmann equilibrium value, a_L and R_{1L} are the fraction and rate constant for the apparent component with the longer T_1 ($T_{1L} = {R_{1L}}^{-1}$), a_S and R_{1S} are the fraction and rate constant for the apparent component with the shorter T_1 ($T_{1S} = {R_{1S}}^{-1}$), and t is the running time for recovery by relaxation. Because a_L and a_S are related ($a_S + a_L = 1$), there are only three independent parameters: R_{1L}, R_{1S}, and a_S (or a_L), expressed as

$$R_{1\mathrm{ex}} = r_1[CA] + R_{1\mathrm{ex}}^0 \quad (3)$$

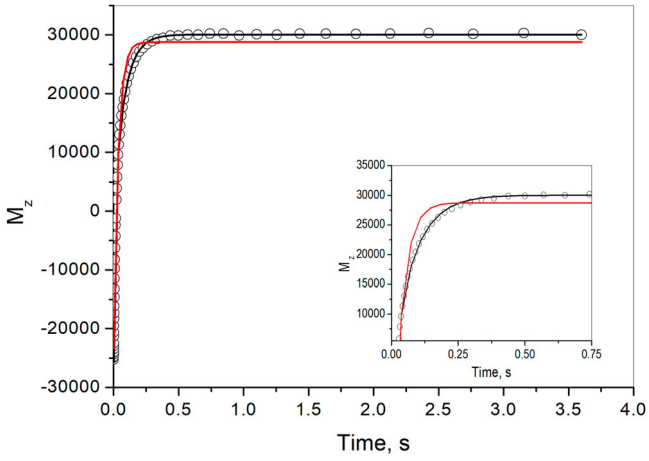

Figure 1. IR data of a TS/A sample in the presence of a 15 mM Gd-HPDO3A solution (21.5 MHz and 25°C). Data were fitted according to the 2SX model (black line, Equation (1)) and the monoexponential recovery (red line, $M_z = M_0(1–2\exp(-t/T_1)) + \text{offset}$).

$$R_{1L} = \frac{1}{2}\left(R_{1in} + R_{1ex} + \tau_{in}^{-1} + \frac{V_{in}}{\tau_{in}(1-V_{in})}\right) - \frac{1}{2}\left[\left(R_{1in} - R_{1ex} + \tau_{in}^{-1} - \frac{V_{in}}{\tau_{in}(1-V_{in})}\right)^2 + \frac{4V_{in}}{\tau_{in}^2(1-V_{in})}\right]^{\frac{1}{2}} \quad (4)$$

$$R_{1S} = \frac{1}{2}\left(R_{1in} + R_{1ex} + \tau_{in}^{-1} + \frac{V_{in}}{\tau_{in}(1-V_{in})}\right) + \frac{1}{2}\left[\left(R_{1in} - R_{1ex} + \tau_{in}^{-1} - \frac{V_{in}}{\tau_{in}(1-V_{in})}\right)^2 + \frac{4V_{in}}{\tau_{in}^2(1-V_{in})}\right]^{\frac{1}{2}} \quad (5)$$

$$a_S = \frac{1}{2}\left(1 - \frac{(R_{1in} - R_{1ex})(1-2V_{in}) + \tau_{in}^{-1} + \frac{V_{in}}{\tau_{in}(1-V_{in})}}{\left[\left(R_{1in} - R_{1ex} + \tau_{in}^{-1} - \frac{V_{in}}{\tau_{in}(1-V_{in})}\right)^2 + \frac{4V_{in}}{\tau_{in}^2(1-V_{in})}\right]^{\frac{1}{2}}}\right) \quad (6)$$

where $R_{1ex}{}^0$ is the extracellular relaxation rate with no CA, [CA] is the millimolar concentration of the CA in the extracellular space and r_1 is its relaxivity value.

The metal complex addition permits the V_{in} and V_{ex} assessment by the measurement of Gd and Eu concentrations by inductively coupled plasma mass spectrometry (ICP-MS; element-2; Thermo-Finnigan, Rodano (MI), Italy). Since the metal complexes distribute only in V_{ex}, the latter was determined following the relationship:

$$V_{ex} = n^{Gd/Eu}(\text{mol})/(M^{Gd/Eu}(\text{mol}/l) * \text{Vol}_p(l)) \quad (7)$$

were $n^{Gd/Eu}$ is the number of Gd or Eu moles determined by ICP-MS; M is the concentration of the M-HPDO3A solution (M = Gd or Eu) added to the cells, and Vol_p is the volume of the wet cellular pellets.

From the experiments carried out in the presence of Eu-HPDO3A, the relaxation rate values of the cytosolic compartment R_{1in} for TS/A was determined equal to 1.10 s^{-1}, performing the fitting of the IR data according to Equation (1), with fixed $R_{1ex}{}^0$ values of 0.4 s^{-1}.

3. Results and discussion

In order to perform a quantitative analysis of water dynamics in the different cell lines and to establish its relationship with the FFC-NMR profile behaviour, the assessment of the cell membrane permeability is crucial. For this reason, a series of R_1 measurements (0.5 T and 25°C) were acquired by adding increasing amounts (15–40 mM) of Gd-HPDO3A to the extracellular space of the TS/A cells grown in normo- and hypoxic conditions, respectively. Hypoxic conditions were obtained by culturing cells in a hypoxia incubator (CO_2 5%, N_2 94%, O_2 1%) for one week. In order to avoid the internalisation of the metal complex, the addition of Gd-HPDO3A was performed at 25°C and the relaxometric investigation was carried out within 15 min. Then, the IR data were analysed according to the two sites (2SX) kinetic model [1,3,4, 20] using, as fitting constraints, the relaxation rate of the intra- and the extracellular compartments in the absence of the paramagnetic probe (1.10 and 0.4 s^{-1}, respectively, see Material and Methods), and the relaxivity of Gd-HPDO3A (4.5 s^{-1} mM^{-1}). The obtained kinetic parameters are reported in Table 1.

The most important result shown in Table 1 is the significant decrease of the residence lifetime of water molecules in cell cytoplasm (τ_{in}) for cell grown under hypoxic conditions. This behaviour is due to the hypoxia induced switch of cells to the glycolytic phenotype. It follows that the change in τ_{in} can be exploited as a

Table 1. The kinetic parameters obtained by fitting the M_z recovery data for TS/A in normo and hypoxia conditions.

TS/A culture condition	Intracellular residual lifetime τ_{in} (s)
Normoxia	0.039 ± 0.012 [4]
Hypoxia	0.013 ± 0.004
W/o Gln	0.095 ± 0.016

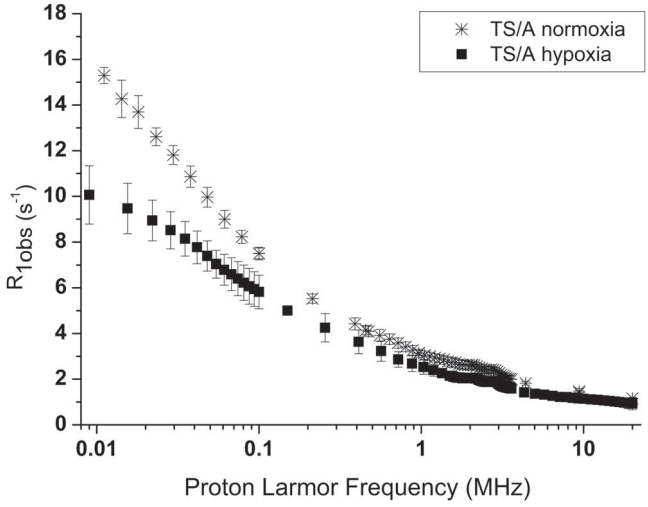

Figure 2. FFC-NMR profiles acquired on TS/A cells grown in normoxic (black stars) and hypoxic (black filled square) conditions. The T_1 were measured at 25°C; the mean ± SD is calculated from at least three independent experiments.

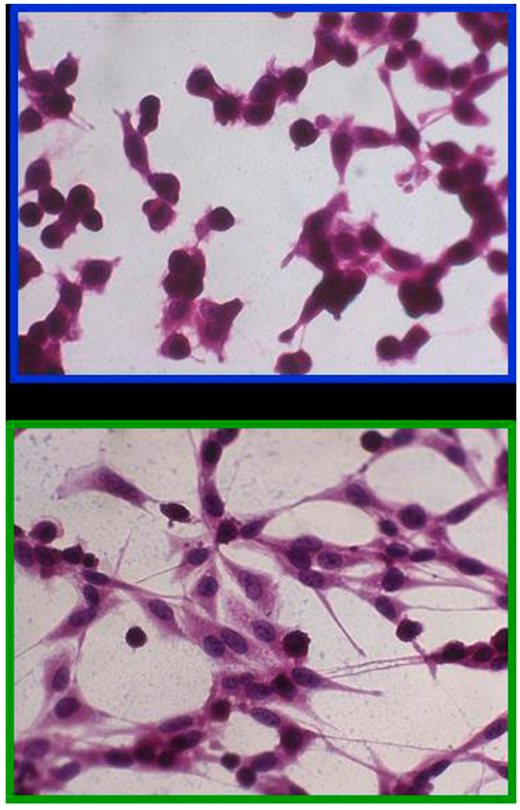

Figure 3. Histology image of TS/A cells grown one week in normoxia (blue panel) and hypoxia (green panel). Cells were stained with haematoxylin and eosin. Magnification 40×. Images evidence the increased cytoplasmatic volume of TS/A grown in hypoxia condition.

biomarker of this metabolic change. Then FFC-NMR profiles of mammary adenocarcinoma cells (TS/A) cultured for 1 week in normoxic or hypoxic conditions were acquired at variable magnetic field strengths ranging from 0.01 to 10 MHz. For the acquisition of the FFC-NMR profile, cells were detached by culture flasks with trypsin, washed with PBS and centrifuged in a 5 mm glass NMR tube to obtain a pellet 0.8–1 cm height after 15 min at 0.2 rcf. The viability of TS/A cells after the acquisition (30 min) of the NMRD profile was determined by trypan blue assay and it resulted to be higher than 85%. The observed dispersion curve (Figure 2) is characteristic of diamagnetic tissue relaxation [21,22]. T_1 values of TS/A cells grown in hypoxia are significantly longer than normoxic one and the differences are inversely proportional to the magnetic field strength (from 40 to 10% in the range 0.01–10 MHz).

The challenging hypothesis is that hypoxia induces cell swelling with a consequent increase in the amount of cytoplasmatic water and its mobility, both changes resulting in longer T_1 values. Cell histology, in particular, H&E staining (Figure 3), confirmed the occurrence of cellular swelling.

To support the view that the R_1 decrease of the $1/T_1$ FFC-NMR profile is directly proportional to the osmotically driven increase of the cytoplasmatic volume, FFC-NMR profiles were acquired for TS/A, grown in normoxic conditions, but incubated (for 10 min) in a hypoosmotic buffer (220 mOsm) prior to undergo to the profile acquisition. Figure 4 shows that the obtained FFC-NMR profile is similar to that of cells grown in hypoxic conditions. From these preliminary data, one may suggest that water exchange through cell membranes can significantly affect the T_1 thus reporting non-invasively on tumour characteristics that are fundamental for correct prognosis and treatment decision.

On the contrary, MR images of cellular pellets acquired at 1 T were unable to distinguish the cell pellets grown in the normo- and hypoxic or in different osmolarity conditions as shown in Figure 5.

With respect to the other methodologies currently proposed for hypoxia imaging, the herein described approach shows many advantages. For example, positron emission tomography (PET) exploits the tracer [^{18}F] fluoromisonidazole ([^{18}F]FMISO) [23,24], for hypoxia molecular imaging. In hypoxic environments, [^{18}F] FMISO radical anion persists long enough to react with macromolecules, trapping the tracer in the intracellular compartment. However, considering the low target-to-background ratio and slow uptake in malignant tissues, the use of [^{18}F]FMISO was quite limited and new tracers are still under scrutiny. On the contrary, the relaxometric method herein described avoids the use

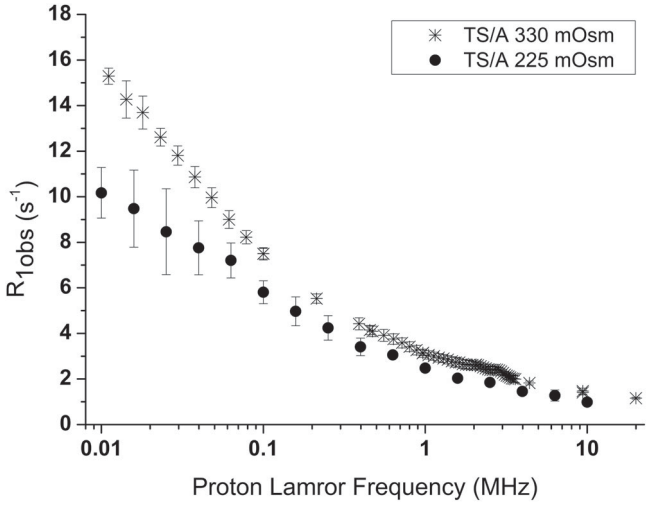

Figure 4. FFC-NMR profiles acquired on TS/A cells grown in normo (330 mOsm, black stars) and hypo osmolar (225 mOsm, black filled circle) conditions. The T_1 were measured at 25°C; the mean ± SD is calculated from at least three independent experiments.

Figure 5. T_1-weighted spin-echo MRI image (measured at 1T) of an agar phantom containing TS/A cells grown in: normoxia, hypoxia, 225 mOsm, medium, 300 mOsm medium (from the left to the right, respectively).

of exogenous tracers being responsive to an endogenous parameter, i.e. the osmotically driven changes of water exchange rate. Oxygen enhanced MRI represents another approach to hypoxia imaging [25]. It is based on the use of molecular oxygen as a contrast agent as it causes a decrease of R_1 after its inhalation. In hypoxic tissue, the inhaled oxygen molecules bind preferentially to deoxygenated haemoglobin molecules, converting the paramagnetic deoxyhaemoglobin to diamagnetic oxyhaemoglobin. Therefore, hypoxic tumour regions can be detected by the absence of measurable positive ΔR_1. The

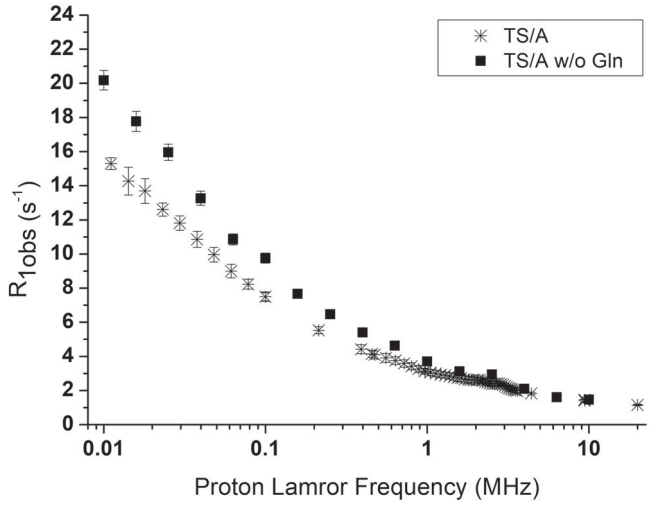

Figure 6. FFC-NMR profiles acquired on TS/A cells grown in the absence (black filled square) and in the presence (4 mM) of Gln (black stars). The T_1 values were measured at 25°C.

main limitation is that ΔR_1 can be strongly influenced by differences in gas delivery and inhalation.

Next, we assessed the change in the metabolism of TS/A cells upon incubation for 24 h at 37°C (CO_2 5%) in a Gln free medium. Figure 6 shows the FFC-NMR profiles acquired for TS/A grown in the presence and in the absence of glutamine for 24 h. As shown in Figure 4, the differences are again inversely proportional to the applied magnetic field strength with an increase of R_{1obs} at low field of ca. 30% in the absence of Gln. The τ_{in} was determined using the fixed field method described above, i.e. in the presence of 5–20 mM Gd-HPDO3A in the extracellular space. Table 1 shows that Gln deprivation causes a significant increase of τ_{in} as a consequence of the decrease of cellular metabolism. Gln is fundamental for highly proliferative cancer cells that use this aminoacid as an essential substrate for energy source, as well as for generation of nucleotides, lipids, and proteins. This result suggests that measurements of water exchange rates can be used to distinguish between tumour and normal cells due to their different response to the change of the amount of Gln present in the growing medium.

4. Conclusions

On the basis of the obtained results, one may conclude that variations of water exchange rates across the intra- and extracellular compartments can be considered as reporters of tumour metabolic status. In fact, water dynamics in breast cancer cells (TS/A) grown in normo- and hypoxic conditions and with and without the presence of glutamine in the incubation medium appears significantly different. This difference can be exploited

to obtain relevant physiological information for a correct diagnosis, treatment decisions and monitoring in oncology.

Moreover, changes in tissue water dynamics can be monitored 'in vitro' and 'in vivo' by measuring FFC-NMR $1/T_1$ dispersion profiles that strongly depend on this parameter. Thus, FFC relaxometry may become a paradigm-shifting technology which will generate new, quantitative disease biomarkers, that will be spatially detected in the images acquired on the FFC-MRI scanners currently developed at Lurie's lab in Aberdeen [26,27].

Disclosure statement

No potential conflict of interest was reported by the authors.

Funding

This project has received funding from the European Union's Horizon 2020 (H2020 Health) research and innovation programme under grant agreement No 668119 (project 'IDentIFY'). This article is based upon work from COST Action EURELAX, CA15209, supported by COST (European Cooperation in Science and Technology).

References

[1] C.S. Springer Jr, J. Magn. Reson. **291**, 110 (2018).
[2] N.J. Ernest and H. Sontheimer, Brain Res. **1144**, 231 (2007).
[3] C.S. Springer Jr, X. Li, L.A. Tudorica, K.Y. Oh, N. Roy, S.Y. Chui, A.M. Naik, M.L. Holtorf, W.D. Afzal, A. Rooney and W. Huang, NMR Biomed. **27**, 760 (2014).
[4] M.R. Ruggiero, S. Baroni, S. Pezzana, G. Ferrante, S. Geninatti Crich and S. Aime, Angew. Chem. Int. Ed. Engl. **57**, 7468 (2018).
[5] C.J. Walsh, A. Lebedev, E. Aten, K. Madsen, L. Marciano and H.C. Kolb, Antioxid. Redox Signal. **21**, 1516 (2014).
[6] S. Matsumoto, S. Kishimoto, K. Saito, Y. Takakusagi, J.P. Munasinghe, N. Devasahayam, C. Hart, R.J. Gillies, J.B. Mitchell and M.C. Krishna, Cancer Res. (2018). doi:10.1158/0008-5472.CAN-18-0491
[7] H.P. Rutz, Cancer Biol Ther. **9**, 812 (2004).
[8] R.A. Gatenby and R.J. Gillies, Nature Rev Cancer. **4**, 891 (2004).
[9] C. Yoon Jin, K. Eun-Sol and K. Ja Seung, Int. J. Mol. Sci. **19**, 907 (2018).
[10] M.G. Dilshara, J.W. Jeong, R.G. Prasad Tharanga Jayasooriya, I.M. Neelaka Molagoda, S. Lee, S.R. Park, Y.H. Choi and G.Y. Kim, Biochem. Biophys. Res. Comm. **485**, 440 (2017).
[11] C. Rozera, D. Carlei, P.L. Lollini, C. De Giovanni, P. Musiani, E. Di Carlo, F. Belardelli and M. Ferrantini, Am. J. Pathol. **154**, 1211 (1999).
[12] M. Giovarelli, P. Musiani, A. Modesti, P. Dellabona, G. Casorati, A. Allione, M. Consalvo, F. Cavallo, F. Di Pierro, C. De Giovanni, T. Musso and G. Forni, J. Immunol. **155**, 3112 (1995).
[13] E. Terreno, S. Geninatti Crich, S. Belfiore, L. Biancone, C. Cabella, G. Esposito, A.D. Manazza and S. Aime, Magn. Reson. Med. **55**, 491 (2006).
[14] E. Gianolio, G. Ferrauto, E. Di Gregorio and S. Aime, Biochim. Biophys. Acta Biomembr. **1858**, 627 (2016).
[15] C. Labadie, J.H. Lee, G. Vtek and C.S. Springer Jr, Magn. Reson. B. **105**, 99 (1994).
[16] C. Bailey, A. Giles, G. Czarnota and G. Stanisz, Magn Reson Med. **62**, 46 (2009).
[17] S. Geninatti Crich, L. Biancone, V. Cantaluppi, D. Duò, G. Esposito, S. Russo, G. Camussi and S. Aime, Magn. Reson. Med. **51**, 938 (2004).
[18] G. Ferrante and S. Sykora, Adv. Inorg. Chem. **57**, 405 (2005).
[19] S. Geninatti-Crich, I. Szabo, D. Alberti, D. Longo and S. Aime, Contrast Media Mol. Imaging. **6**, 421 (2011).
[20] G.J. Wilson, M. Woods, C.S. Springer Jr, S. Bastawrous, P. Bhargava and J.H. Maki, Magn. Reson. Med. **72**, 1746 (2014).
[21] S.H. Koenig, Acad Radiol. **3**, 597 (1996).
[22] Y. Gossuin, C. Burtea, A. Monseux, G. Toubeau, A. Roch, R.N. Muller and P. Gillis, J Magn Reson Imaging. **20**, 690 (2004).
[23] K. Miyake, D. Ogawa, M. Okada, T. Hatakeyama and T. Tamiya, Neurol Med Chir (Tokyo). **56**, 396 (2016).
[24] Z. Xu, X.F. Li, H. Zou, X. Sun and B. Shen, Oncotarget. **8**, 94969 (2017).
[25] A. Ross, et al., Radiology. **288**, 739 (2018).
[26] P.J. Ross, L.M. Broche and D.J. Lurie, Magn. Reson. Med. **73**, 1120 (2015).
[27] L.M. Broche, G.P. Ashcroft and D.J. Lurie, Magn. Reson. Med. **68**, 358 (2012).